Evidence for an interaction of the metalloprotease–disintegrin tumour necrosis factor α convertase (TACE) with mitotic arrest deficient 2 (MAD2), and of the metalloprotease–disintegrin MDC9 with a novel MAD2-related protein, MAD2β

Karen K. NELSON*[1], Johannes SCHLÖNDORFF*†[1] and Carl P. BLOBEL*[2]

*Cellular Biochemistry and Biophysics Program, Sloan-Kettering Institute, Memorial Sloan-Kettering Cancer Center, New York, NY 10021, U.S.A., and †Tri-Institutional (Cornell/Rockefeller University/Memorial Sloan-Kettering Cancer Center) MD/PhD Training Program, New York, NY 10021, U.S.A.

Metalloprotease–disintegrins are a family of transmembrane glycoproteins that have a role in fertilization, sperm migration, myoblast fusion, neural development and ectodomain shedding. In the present study we used the yeast two-hybrid system to search for proteins that interact with the cytoplasmic domain of two metalloprotease–disintegrins, tumour necrosis factor α convertase (TACE; ADAM17) and MDC9 (ADAM9; meltrin γ). We have identified mitotic arrest deficient 2 (MAD2) as a binding partner of the TACE cytoplasmic domain, and a novel MAD2-related protein, MAD2β, as a binding partner of the MDC9 cytoplasmic domain. MAD2β has 23% sequence identity with MAD2, which is a component of the spindle assembly (or mitotic) checkpoint mechanism. Northern blot analysis of human tissues indicates that MAD2β mRNA is expressed ubiquitously. The interaction of the TACE and MDC9 cytoplasmic domains with their binding partners has been confirmed biochemically. The independent identification of MAD2 and MAD2β as potential interacting partners of distinct metalloprotease–disintegrins raises the possibility of a link between metalloprotease–disintegrins and the cell cycle, or of functions for MAD2 and MAD2β that are not related to cell cycle control.

Key words: ADAMs, MAD2, MDC9, TACE, yeast two-hybrid screen.

INTRODUCTION

Metalloprotease–disintegrins (also referred to as ADAMs or MDC proteins) are transmembrane glycoproteins with a characteristic domain organization composed of a signal sequence, pro-, metalloprotease and disintegrin domains, a cysteine-rich region, a transmembrane domain and a cytoplasmic tail [1,2]. This protein family, which now includes over 27 members, has been implicated in a number of cellular processes (reviewed in [1–3]). These include a role in fertilization [4–14], sperm migration [12], myoblast fusion [15] and specific developmental processes [16], including those mediated by Notch [17–20] and transforming growth factor α [21]. The protease responsible for releasing tumour necrosis factor α (TNF-α) from cellular membranes, tumour necrosis factor α convertase (TACE), was recently identified as a metalloprotease–disintegrin protein [22,23]. TACE has now also been implicated in the ectodomain shedding of various other proteins, including transforming growth factor α, p75 tumour necrosis factor receptor, L-selectin [21] and the amyloid precursor protein [24,25]. Recent evidence suggests that the metalloprotease–disintegrin MDC9 is involved in shedding the heparin-binding epidermal growth factor-like growth factor [26].

The ectodomain shedding of numerous proteins seems to be regulated. The TACE-mediated release of TNF-α from cells is up-regulated by various stimuli, such as lipopolysaccharide and phorbol esters [22,27,28], and TACE seems to be the major regulated amyloid precursor protein α-secretase activity [24,25]. Several metalloprotease–disintegrins contain potential signalling motifs such as SH3 ligand domains and protein kinase C phosphorylation sites in their cytoplasmic domains. MDC9 is phosphorylated after the addition of PMA to cells [29] and apparently interacts with protein kinase Cδ [26]. Furthermore, sequences within the cytoplasmic tail of *Drosophila* Kuzbanian seem to be important for mediating the dominant-negative effects of a truncated form of the protein [18].

To identify cytoplasmic proteins that might be involved in the regulation of metalloprotease–disintegrin activity, we searched for binding partners that interact with the cytoplasmic domain of two metalloprotease–disintegrins, TACE and MDC9. By using a yeast two-hybrid screen, we have identified mitotic arrest deficient 2 (MAD2) as a binding partner of the TACE cytoplasmic domain and MAD2β, a novel MAD2-related protein, as a binding partner of the MDC9 cytoplasmic domain. MAD2 is a component of the spindle assembly (or mitotic) checkpoint mechanism and is conserved from yeast to humans [30–33]. MAD2β has 23% sequence identity with MAD2, and MAD2β mRNA is expressed ubiquitously. We have mapped the regions of TACE and MDC9 cytoplasmic domains sufficiently for mediating their respective interactions with MAD2 and MAD2β and have confirmed both interactions *in vitro*. In addition, the interaction of TACE with MAD2 has been confirmed in COS-7

Abbreviations used: APC, anaphase-promoting complex; FLAG, Asp-Tyr-Lys-Asp-Asp-Asp-Asp-Lys; GST, glutathione S-transferase; MAD2, mitotic arrest deficient 2; TACE, tumour necrosis factor α convertase.

[1] These authors contributed equally to this work.

[2] To whom correspondence should be addressed (e-mail c-blobel@ski.mskcc.org).

cells. These observations suggest that MAD2 and the related novel protein MAD2β might have a role in regulating the function of metalloprotease–disintegrins, or vice versa.

EXPERIMENTAL

Reagents

All reagents were obtained from Sigma unless indicated otherwise. [α-^{32}P]dCTP used for the labelling of cDNA probes was purchased from NEN Life Science Products.

Expression vectors

cDNA fragments coding for various segments of the TACE cytotail (see Figure 2C) were generated from a human TACE cDNA clone (kindly provided by Dr. J. D. Becherer) by PCR. Primers were designed such that the resulting fragments contained a 5′ *Eco*RI restriction site and a 3′ stop codon and *Sal*I restriction site. For use in the yeast two-hybrid system, the resulting TACE fragments were cloned in frame to the *GAL4* DNA-binding domain of the pGBT9 vector (Clontech). Plasmids encoding fusion proteins of glutathione S-transferase (GST) and the TACE cytotail regions were obtained by inserting the same TACE cDNA fragments into the pGEX-4T-1 vector (Pharmacia). Similarly, plasmids coding for various segments of the MDC9 cytoplasmic tail were generated by PCR (see Figure 6B). All MDC9 fragments were synthesized such that they contained a 5′ *Eco*RI site, and a 3′ stop codon and *Sal*I site. These fragments were cloned in frame to the *GAL4* DNA-binding domain of the pGBT9 vector for yeast two-hybrid analysis, or into the pGEX-4T-3 vector (Pharmacia) for expression of the GST fusion protein (GST–MDC9) containing the entire cytoplasmic tail of MDC9 (residues 719–819).

The cytoplasmic tails of the metalloprotease–disintegrins human MADM (ADAM 10) residues 697–748, mouse meltrin α (ADAM 12) residues 728–903, human MDC 15 (ADAM 15) residues 712–814, and mouse meltrin β (ADAM 19) residues 725–920 were also generated by PCR with gene-specific primers and were subsequently inserted in frame into the pGBT9 vector. All constructs were sequenced for potential PCR-generated mutations. Residues are as designated in the GenBank Nucleotide Sequence Database [accession numbers U41766 (MDC9), AF009615 (MADM), D50411 (meltrin α), U41767 (MDC15), U86755 (TACE) and AF019887 (meltrin β)].

Full-length hsMAD2 cloned into both the pET28a (Novagen) and pFLAG-CMV2 vectors (Eastman Kodak) was kindly provided by Dr. K. Wassman, Dr. Y. Li and Dr. R. Benezra. For MAD2β, the entire 1 kb *Eco*RI–*Xho*I insert from the original two-hybrid clone was inserted into the pFLAG-CMV2 and the pET28b vectors to produce plasmids encoding FLAG-tagged (in which FLAG is Asp-Tyr-Lys-Asp-Asp-Asp-Asp-Lys) and T7-His-tagged MAD2β respectively.

Yeast two-hybrid screen

The Clontech Matchmaker Two-Hybrid System was used for both the TACE and MDC9 cytotail screens. In brief, the full-length cytoplasmic tails of MDC9 (residues 719–819) and TACE (residues 695–824) were cloned into pGBT9 to yield in-frame fusions with the *GAL4* DNA-binding domain. The yeast reporter strain HF7c (MAT **a** *ura3-52*, *his3-200*, *lys2-801*, *ade2-101*, *trp1-901*, *leu2-3*, *112*, *gal4-542*, *gal80-538*, *LYS2::GAL1-HIS3*, *URA3::*(*GAL4 17 mers*)$_3$-*CYC1-lacZ*) was co-transformed with a human HeLa cDNA library cloned into the pGAD GH vector, downstream of the *GAL4* activation domain (Clontech) and either pGBT9-TACE or pGBT9-MDC9. Both MDC9 and TACE are widely expressed, including in HeLa cells (results not shown). In accordance with the supplier's recommendations, *HIS3* gene expression was assessed by growth on histidine-free media, whereas *lacZ* gene expression was determined with a colorimetric filter assay. cDNA clones from colonies positive by both histidine prototrophy and β-galactosidase activity were isolated, transferred into XL1 Blue bacteria and identified by cDNA sequencing (Sequenase; USB). The specificity of the interactions was tested by co-transforming potential positive plasmids with the control vectors pGBT9 and pLAM 5′ (Clontech), which respectively encode the *GAL4* DNA-binding domain and the *GAL4* DNA-binding domain fused to human lamin C. Plasmid isolation and all further manipulations in yeast were performed with protocols recommended by the manufacturer (Clontech).

In the MDC9 screen, three clones encoding a novel MAD2-related protein, termed MAD2β, were isolated. All three clones coded for a protein of 211 amino acid residues. An in-frame stop codon upstream of the predicted start codon was not present in any of the three clones isolated (the longest 5′ untranslated region was 54 bp). One cDNA clone was sequenced entirely on both strands and used in all further manipulations (accession number AF072933). The start codon indicated in Figure 4 is likely to be the correct start of translation because there is good agreement between the size of the mRNA on a Northern blot and the length of the cDNA insert, and between the apparent molecular mass of the protein by SDS/PAGE and the predicted molecular mass. Furthermore, the position of the initial methionine residue of MAD2β is similar to the position of the initial methionine residue of MAD2 in an alignment of both proteins (see Figure 4).

Antibody production

A GST fusion protein containing the entire TACE cytoplasmic tail (residues 695–824) was expressed and purified from BL21 bacteria as described previously [34] and used as an immunogen to raise rabbit polyclonal antisera. Polyclonal anti-hsMAD2 antibodies were a gift from Dr. Y. Li and Dr. R. Benezra. The anti-FLAG M2 monoclonal antibody was purchased from Sigma. The anti-T7 Tag monoclonal antibody was purchased from Novagen.

Northern blot analysis

Multiple tissue Northern blots were purchased from Clontech. The MAD2β probe (an *Eco*RI–*Sty*I fragment corresponding to the entire coding region) was ^{32}P-labelled with the Prime-It II random primer labelling kit (Stratagene) followed by purification with a MicroSpin S-400 HR column (Pharmacia). High-stringency hybridization with ExpressHyb and washes were performed in accordance with Clontech's recommendations. Human β-actin cDNA probe (Clontech) was used as a control to ensure comparable mRNA loading for different tissues.

Binding assays *in vitro*

Recombinant hsMAD2, containing a hexahistidine tag, was purified as described previously [30]. GST–TACE-cytotail fusion proteins were overexpressed in BL21 *Escherichia coli*, and the cells were lysed in PBST [PBS, pH 7.4, with 1 % (v/v) Triton X-100 and protease inhibitors [6]] by three freeze–thaw cycles followed by a 13000 ***g*** spin for 20 min. Equal amounts of lysate were preincubated with glutathione–Sepharose 4B beads (Pharmacia) in PBST for 20 min before the addition of purified

recombinant His-tagged hsMAD2 to a final concentration of 2 μg/ml. After incubation for 2 h at 4 °C, the beads were washed three times in PBST. Bound material was eluted at 95 °C for 5 min in sample loading buffer and separated by SDS/PAGE. Samples were analysed by Ponceau staining followed by Western blotting, essentially as in [35], with anti-MAD2 antibodies.

For MAD2β binding studies, GST or GST–MDC9 was expressed in bacteria and purified on glutathione–Sepharose 4B beads, essentially as described in [36]. The beads saturated with either fusion protein were incubated with cell lysates from COS-7 cells overexpressing FLAG-tagged MAD2β. Cell lysates were prepared as described for immunoprecipitations. The lysates and beads were incubated overnight at 4 °C. After three washes with lysis buffer, the proteins that co-precipitated with MDC9 or control GST proteins were eluted at 95 °C for 5 min in sample loading buffer. Samples were analysed by SDS/PAGE followed by immunoblotting with anti-FLAG M2 monoclonal antibodies (Sigma).

To demonstrate direct binding of MAD2β, T7–His-tagged MAD2β fusion protein was overexpressed in BL21 *E. coli* and bacterial lysates were prepared as described above. Glutathione–Sepharose 4B beads saturated with either GST or GST–MDC9 (prepared as described above) were incubated overnight with these bacterial lysates at 4 °C. After three washes with lysis buffer, bound proteins were eluted at 95 °C for 5 min in sample loading buffer. Samples were analysed by SDS/PAGE followed by immunoblotting with anti-T7 Tag monoclonal antibodies (Novagen).

Cell culture, transfection and immunoprecipitation

COS-7 cells (A.T.C.C., Manassas, VA, U.S.A.) were maintained in Dulbecco's modified Eagle's medium supplemented with 5% (v/v) fetal bovine serum, glutamine, 100 i.u./ml penicillin G and 100 μg/ml streptomycin. All constructs were transfected into COS-7 cells grown in six-well tissue culture plates (Falcon) with LipofectAMINE (Life Technologies). At 2 days after transfection, cells were washed in PBS and lysed in 500 μl of lysis buffer [containing 0.5% (v/v) Nonidet P40, Tris-buffered saline, pH 7.4, and protease inhibitors] in each well. Lysates were spun at 13000 ***g*** for 15 min. A small volume of each lysate was mixed with an equal volume of 2 × sample loading buffer and used to assay for protein expression by Western blotting. The remaining lysates were incubated with anti-(TACE cytotail) polyclonal antibody (2 μl of serum per ml of lysate) and rProtein A–Sepharose Fast Flow beads (Pharmacia) for 2 h at 4 °C. After four washes in lysis buffer, protein bound to the beads was eluted in sample loading buffer for 5 min at 95 °C. Samples were analysed by Western blotting as described [35].

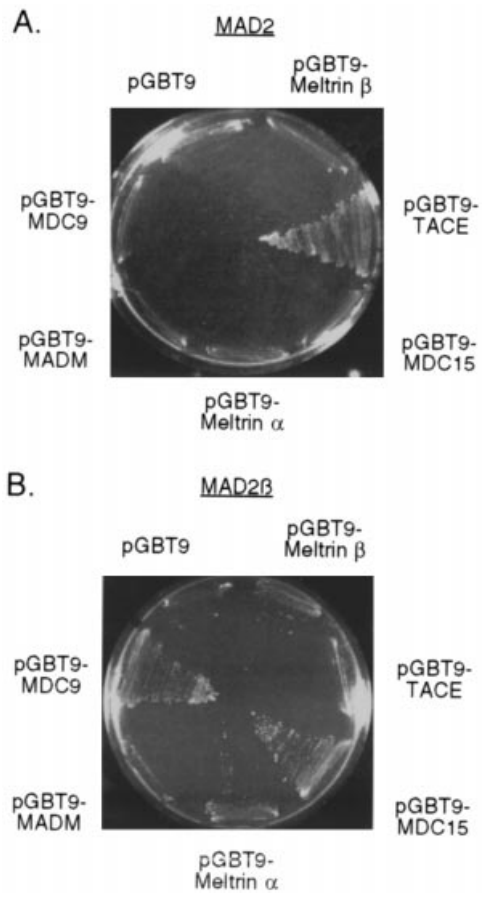

Figure 1 Analysis of the interaction of MAD2 and MAD2β with different metalloprotease–disintegrin proteins by means of the yeast two-hybrid system

The yeast reporter strain HF7c was co-transformed with the cytoplasmic tails of various metalloprotease–disintegrins fused to the *GAL4* DNA-binding domain of pGBT9 and with either full-length human MAD2 fused to the *GAL4* activation domain of the pGAD GH vector (**A**) or with full-length MAD2β fused to the *GAL4* activation domain of pGAD GH (**B**). Colonies were streaked on plates lacking histidine and incubated at 30 °C for 3 days. The metalloprotease–disintegrins tested were MDC 9 (meltrin γ; ADAM 9), MADM (KUZ; ADAM 10), meltrin α (ADAM 12), MDC 15 (ADAM 15), TACE (ADAM 17) and meltrin β (ADAM 19). pGBT9 indicates the parental vector, which expresses the *GAL4* DNA-binding domain alone. Identical results were obtained when the co-transformants were assayed by colorimetric filter assay to detect the expression of the *lacZ* gene and all co-transformants grew well on plates containing histidine (results not shown).

RESULTS

Interaction of MAD2 with TACE and of MAD2β, a novel MAD2-related protein, with MDC9 in the yeast two-hybrid system

The cytoplasmic tail of TACE and the cytoplasmic tail of MDC9 were used as bait in two separate two-hybrid screens to identify interacting partners from a HeLa cDNA library. It is important to note that bait proteins are usually not phosphorylated in a yeast two-hybrid screen, so that most probably only proteins that interact with MDC9 or TACE independently of potential cytoplasmic tail phosphorylation will be identified. On the basis of both nutritional selection and β-galactosidase activity, 31 clones of MAD2 were isolated by an interaction with the TACE cytotail, and three clones of a novel MAD2-related protein, termed MAD2β (see Figure 4), were isolated by an interaction with the MDC9 cytoplasmic domain. In addition, two SH3-domain containing proteins were isolated as potential binding partners for MDC9 [36a]. Under identical conditions, both MAD2 and MAD2β were unable to interact with the negative control, human lamin C (results not shown), or the *GAL 4* DNA-binding domain alone (Figure 1). For MAD2, numerous cDNA clones contained the entire coding region, whereas the shortest MAD2 cDNA isolated in the screen began with residue 8. All clones included the entire C-terminal portion of the protein. All three cDNA clones of MAD2β apparently contained the entire coding region, with varying amounts of upstream sequence (see the Experimental section).

The ability of MAD2 and MAD2β to interact with other metalloprotease–disintegrins was examined as a control for the specificity of these interactions. The cytoplasmic tails of six

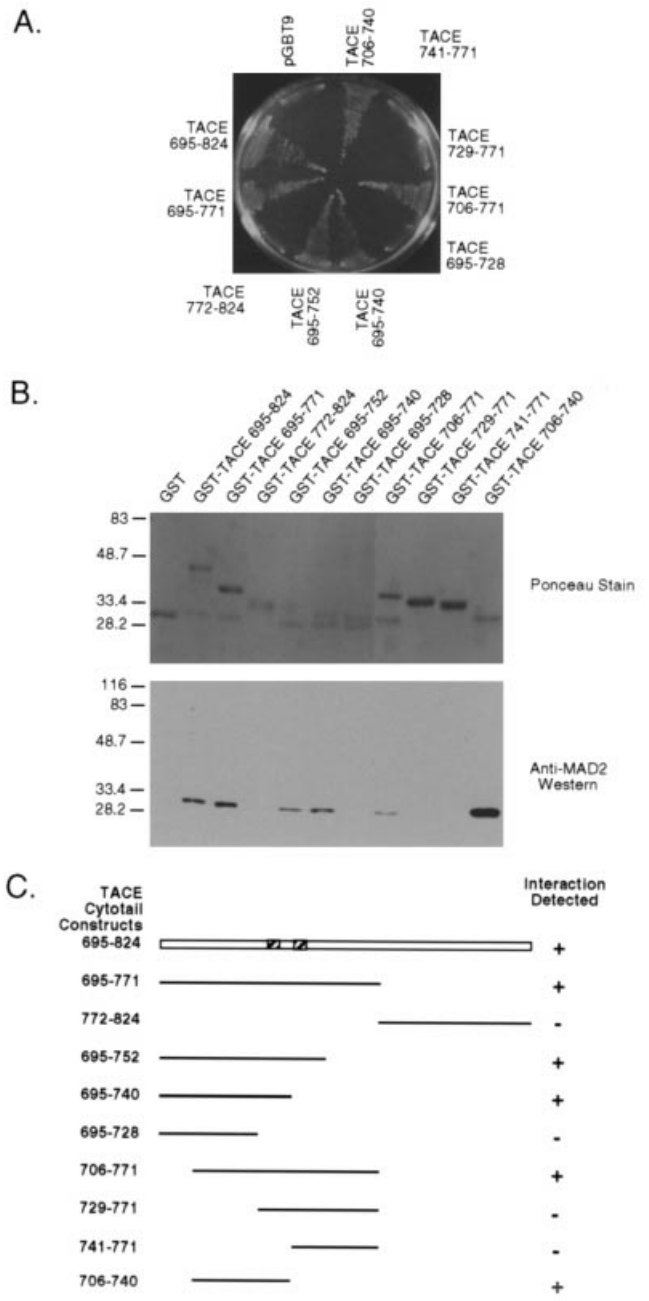

Figure 2 Residues 706–740 of the TACE cytotail are sufficient for the binding of MAD2 in the yeast two-hybrid system and *in vitro*

(**A**) Sector growth assay. The yeast reporter strain HF7c was co-transformed with plasmids encoding the full-length MAD2 fused to the *GAL4* activation domain and various fragments of the TACE cytoplasmic tail fused to the *GAL4* DNA-binding domain. Colonies were streaked on plates lacking histidine and grown at 30 °C for 3 days. All strains grew on plates that contained histidine (results not shown). The numbers indicate the residues of TACE fused to the *GAL4* DNA-binding domain [see (**C**)]. (**B**) MAD2 binds the TACE cytotail *in vitro*. Lysate from bacteria overexpressing either GST or GST fused to various segments of the TACE cytotail were preincubated with glutathione beads, after which purified recombinant MAD2 was added. After incubation with MAD2, the beads were washed and bound material was separated by SDS/PAGE, transferred to nitrocellulose, stained with Ponceau-S (top panel) or Western blotted with an anti-MAD2 polyclonal antibody (lower panel). Staining with Ponceau-S was used to reveal the GST fusion protein but was not sufficiently sensitive to detect the MAD2 protein. The positions of molecular mass markers are indicated (in kDa) at the left. (**C**) Summary of TACE cytotail deletion constructs used and their ability to interact with MAD2. The diagram represents the relative size and location of the TACE sequences fused to the *GAL4* DNA-binding domain and GST for use in the yeast two-hybrid assay and the binding assay *in vitro* respectively. Numbers are amino acid residues. Hatched boxes indicate the locations of the two proline-rich regions. The right panel indicates whether the construct was capable of binding MAD2, as monitored both by nutritional selection and a β-galactosidase assay in yeast [see (**A**), and results not shown] and by the ability to co-precipitate purified MAD2 *in vitro* [see (**B**)].

metalloprotease–disintegrins, MDC9 (ADAM9; meltrin γ), MADM (ADAM10; KUZ), meltrin α (ADAM12), MDC15 (ADAM15; Metargidin), TACE (ADAM17) and meltrin β (ADAM19) were tested for their ability to interact with MAD2 or MAD2β by assessing the interaction-dependent expression of both the nutritional marker gene, *HIS3* (Figure 1), and the *lacZ* gene (results not shown). On the basis of both criteria, only the TACE cytotail was able to interact with MAD2 (Figure 1A). On the basis of both the growth on selective plates (Figure 1B) and the β-galactosidase patch assay, MDC9 interacted robustly with MAD2β. However, MAD2β was also able to interact with MDC15 and weakly with meltrin β, as observed by slow growth on selective plates (Figure 1B) as well as a light blue colour in the β-galactosidase patch assay (results not shown).

Analysis of the interaction of TACE with MAD2

To define the sequence within the TACE cytoplasmic domain responsible for the interaction with MAD2, plasmids coding for various segments of the TACE cytotail fused to the *GAL4* DNA-binding domain were co-transformed into yeast with a plasmid encoding for the *GAL4* activation domain fused to the full-length coding sequence of MAD2. As assayed by nutritional selection (Figure 2A), all constructs containing at least residues 706–740 of TACE bound to MAD2. In contrast, MAD2 did not interact with any of the TACE constructs that did not include the entire 35-residue sequence between residues 706 and 740. A proline-rich putative SH3 ligand domain (PXPXXP) is present within the sequence that is sufficient for MAD2 binding. However, a region N-terminal to it is also required for the interaction (compare constructs 706–771 and 729–771). Comparable results were obtained when β-galactosidase activity was used as an indicator of protein interaction in the yeast two-hybrid system (results not shown). The sequence in TACE that binds MAD2 has no obvious similarity to the binding sites of other known MAD2-binding proteins such as MAD1, insulin receptor or Slp1/Cdc20/p55cdc [37–40].

To establish that the interaction between MAD2 and TACE is direct, we used a biochemical binding assay *in vitro*. Recombinant MAD2 purified from bacteria was incubated with bacterial lysate containing either GST or GST fused to various segments of the TACE cytoplasmic tail. The GST fusion proteins were bound to glutathione beads and their ability to co-precipitate MAD2 was assessed by Western blot analysis. As shown in Figure 2(B), the fusion protein of full-length TACE cytotail with GST, but not GST alone, bound to MAD2. Furthermore, various GST constructs containing only partial TACE cytotail sequence behaved identically with their two-hybrid counterparts in terms of binding to MAD2 (Figures 2B and 2C). These results indicate that MAD2 binds directly to the TACE cytotail *in vitro* and that the region of TACE spanning residues 706–740 is sufficient for this interaction.

Interaction of TACE and MAD2 in cells

To confirm the existence of a complex between MAD2 and TACE in a cellular context, we expressed an N-terminal FLAG-tagged form of MAD2 in COS-7 cells. Figure 3(A) shows that significant levels of TACE could be detected in COS-7 cells by

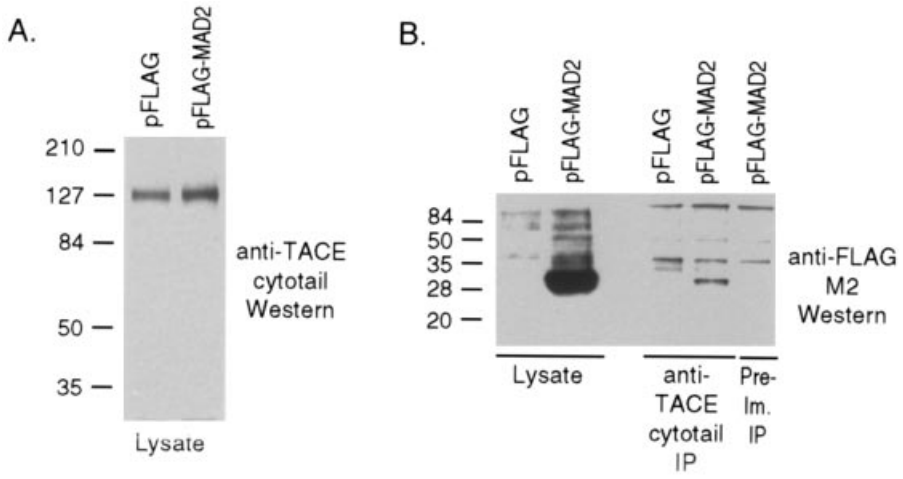

Figure 3 MAD2 interacts with TACE in cells

COS-7 cells were transiently transfected with either control vector (pFLAG) or with a vector encoding full-length MAD2 with an N-terminal FLAG tag (pFLAG–MAD2). (**A**) Similar levels of endogenous TACE were detected by Western blot analysis of both lysates by using antisera raised against the human TACE cytotail. (**B**) Lysates from both cells were also analysed directly by anti-FLAG Western blotting to control for expression of the MAD2 construct (Lysate). Lysates from control and MAD2-overexpressing cells were immunoprecipitated either with anti-TACE cytotail antibody (anti-TACE cytotail IP) or with pre-immune serum (Pre-Im. IP) and the bound material was analysed by Western blotting with the anti-FLAG M2 monoclonal antibody. The positions of molecular mass markers are indicated (in kDa) at the left of each panel.

```
1   MT-TLTRQDLNFGQVVADVLCEFLEVAVHL MAD2ß
1   MALQLSREQGITLRGSAEIVAEFFSFGINS hsMAD2

30  ILYVREVYPVGIFQKRKKYNVPVQMSCHPE MAD2ß
31  TLYQRGIYESETFTRVQKYGLTLLVTTDLE hsMAD2

60  LNQYIQDTLHCVKPLLEKNDVEKVVVILD MAD2ß
61  IIKYLNNVVEQLKDWLYKCSVQKLVVVIS N hsMAD2

90  KEHRPV-EKFVFEITQPPLLSISSDSL MAD2ß
91  IESGEVLERWQFDIECDKTAKDDSAPREKS hsMAD2

116 LSHVEQLLRAFILKISVCDAVLDHNPPGCT MAD2ß
121 QKAIQDEIRSVIRQITATVTFLPLLEVSCS hsMAD2

146 FTVLVHTREAATRNMEKIQVIKDFPWILAD MAD2ß
151 FDLIIYT---------DKDLVVPE-KWEESG hsMAD2

176 EQDVHMHDPRLIPLKTMTSDILKMQLYVEE MAD2ß
172 PQ--FITNSEEVRLRSFTTTIHKVNSMVAY hsMAD2

206 RAHKGS                         MAD2ß
200 KIPVND                         hsMAD2
```

Figure 4 Alignment of the amino acid sequences of MAD2 and MAD2β

The complete amino acid sequences of human MAD2 (accession number U31278) and MAD2β were aligned by the clustal method by using DNAstar MEGALIGN. The amino acid sequences are 23% identical (identical amino acids are boxed).

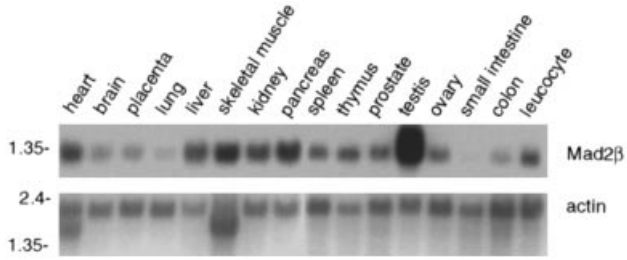

Figure 5 Northern blot analysis of the expression of MAD2β in different tissues

Upper panel: human tissues (Clontech human tissue Northern blots 1 and 2) were probed under high stringency with a ^{32}P-labelled human MAD2β cDNA probe. Lower panel: the quantity and integrity of mRNA present on filters were verified by probing for actin transcripts. The mRNA tissue source is indicated above each lane.

using a polyclonal antiserum raised against the cytoplasmic tail of human TACE. In MAD2-transfected cell lysates immunoprecipitated with an anti-(TACE cytotail) antibody, a band that co-migrated with FLAG-tagged MAD2 was recognized by an anti-FLAG monoclonal antibody (Figure 3B). This protein was not present in lysate immunoprecipitated with pre-immune sera or in lysates from cells transfected with control vector (Figure 3B). Similar results were obtained in co-transfection experiments in which a truncated form of human TACE containing the transmembrane and cytoplasmic tail of the protein, but lacking most of the extracellular structures, was expressed together with FLAG-tagged MAD2. In these experiments, the truncated form of TACE co-immunoprecipitated with FLAG–MAD2 by using the anti-FLAG M2 monoclonal antibody (results not shown).

cDNA sequence and tissue distribution of MAD2β

The cDNA sequence coding for the novel MAD2β protein that interacted with MDC9 revealed that it contained 211 amino acid residues and had a predicted molecular mass of 24 kDa (Figure 4). Furthermore, MAD2β had 23% sequence identity with MAD2 (Figure 4). Northern blot analysis (Figure 5) demonstrated that the 1.35 kb MAD2β mRNA was expressed in all tissues but was most abundant in testis.

Analysis of the interaction of MAD2β with MDC9

To define more closely the sequences within the MDC9 cytoplasmic tail that are necessary for binding to MAD2β, various

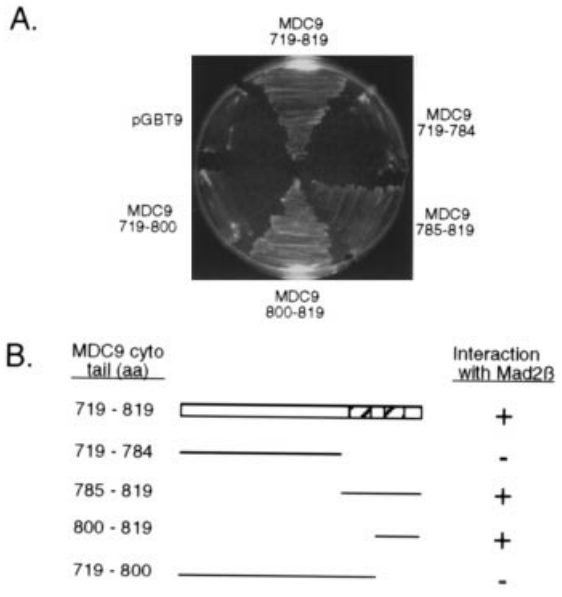

Figure 6 Residues 800–819 of the MDC9 cytotail are sufficient for the binding of MAD2β in the yeast two-hybrid system

(**A**) Sector growth assay. The yeast reporter strain HF7c was co-transformed with plasmids encoding various fragments of the MDC9 cytoplasmic tail fused to the *GAL4* DNA-binding domain and full-length MAD2β fused to the *GAL4* activation domain. Co-transformants were streaked on plates lacking histidine and incubated at 30 °C for 3 days. All strains grew on plates that contained histidine (results not shown). The amino acids encoded by each MDC9 cytotail deletion construct are indicated. (**B**) Summary of MDC9 cytotail deletion constructs and their ability to interact with MAD2β. With the use of the yeast two-hybrid system, various regions of the MDC9 cytotail (shown schematically; numbers refer to amino acid residues) were tested for interaction with MAD2β. A + indicates growth on plates lacking histidine [see (**A**)] as well as a blue colour in the β-galactosidase patch assay (results not shown). Hatched boxes indicate the two proline-rich regions present in the MDC9 cytotail.

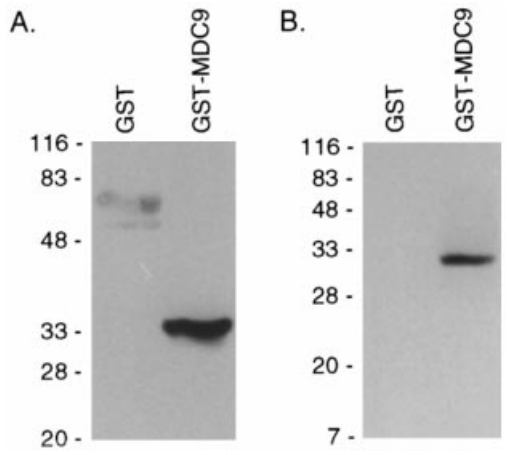

Figure 7 Interaction of MAD2β and MDC9 *in vitro*

(**A**) Glutathione–Sepharose beads saturated with GST or GST–MDC9-cytotail were incubated with lysates derived from COS-7 cells overexpressing FLAG-tagged MAD2β. After incubation with the lysates, the beads were washed; the co-precipitating proteins were eluted and then analysed by Western blot analysis with anti-FLAG monoclonal antibodies. (**B**) To show a direct interaction between MAD2β and MDC9, glutathione–Sepharose beads saturated with GST or GST–MDC9-cytotail were also incubated with lysates derived from bacterial cells overexpressing T7-His-tagged MAD2β. After incubation with the lysates, the beads were washed; the co-precipitating proteins were eluted and then analysed by Western blot analysis with anti-T7 Tag monoclonal antibodies. The positions of molecular mass markers are indicated (in kDa) at the left.

segments of the MDC9 tail were tested for interaction with full-length MAD2β by using the yeast two-hybrid assay, essentially as outlined above for the interaction between TACE and MAD2. The interaction was evaluated by nutritional selection (Figure 6A) as well as by a β-galactosidase assay (results not shown). Both assays indicated that residues 800–819 of MDC9, which also contain a proline-rich putative SH3-ligand domain [36], were sufficient for binding to MAD2β (Figure 6B).

We next analysed the interaction between MAD2β and MDC9 by using two binding assays *in vitro*. First, glutathione–Sepharose beads saturated with GST or GST–MDC9 were added to lysates from COS-7 cells overexpressing FLAG-tagged MAD2β. As shown in Figure 7(A), MAD2β co-precipitated with GST–MDC9 but not with GST alone. These results suggest that MAD2β and MDC9 could form a complex in a whole cellular extract. In the second binding assay, glutathione–Sepharose beads saturated with GST or GST–MDC9 were added to bacterial lysates overexpressing T7-His-tagged MAD2β. The ability of the GST fusion proteins to co-precipitate MAD2β was assessed by Western blot analysis. As shown in Figure 7(B), MAD2β bound to MDC9 cytotail fused to GST but not to GST alone. These results show the direct interaction of MAD2β with the MDC9 cytotail.

DISCUSSION

Here we identify the cell-cycle checkpoint protein MAD2 as a potential binding partner for TACE, and a novel MAD2-related protein, termed MAD2β, as a potential binding partner for MDC9. In both cases the interaction was first established by using the yeast two-hybrid system and then confirmed *in vitro* with proteins isolated from *E. coli*. The TACE/MAD2 interaction was also confirmed in COS-7 cells by the co-immunoprecipitation of MAD2 with antibodies against the TACE cytotail. The binding site for MAD2 in TACE has been narrowed to a 35-residue region of the TACE cytotail, whereas the MAD2β-binding site is within the last 20 residues of the MDC9 cytotail. Interestingly, these binding sites in TACE and MDC9 are proline-rich and contain potential SH3 ligand-binding domains. In MDC9 the proline-rich sequences have been shown to interact with the SH3 domain of Src *in vitro* [36]; furthermore they interact with at least two SH3-domain-containing proteins, endophilin I and SH3PX1, in cells [36a]. Because no discernible SH3 domain is evident in MAD2 or MAD2β, this raises the possibility that MAD2 and MAD2β might compete with or regulate the binding of putative SH3-containing proteins to the cytoplasmic tail, or vice versa.

The association of MAD2 with TACE raises the intriguing possibility of functional interactions between a metalloprotease–disintegrin and mitotic checkpoint control mechanisms. MAD2 is a component of the spindle assembly (or mitotic) checkpoint mechanism and localizes to unattached kinetochores during prometaphase [30,31,41,42]. The spindle assembly checkpoint ensures that anaphase does not begin until all kinetochores have properly attached to the spindle apparatus and are under tension. Recent studies in fission and budding yeast, and in vertebrates, have demonstrated that MAD2 is capable of forming a complex with the anaphase-promoting complex (APC) regulator Slp1/Cdc20/p55Cdc, as well as with the APC itself [32,39,40,43–46]. The APC is responsible for ubiquitinating key cell-cycle regulatory proteins, which targets them for degradation by the 26 S proteosome, thereby allowing exit from mitosis. The binding of MAD2 to the Cdc20–APC complex seems to inhibit the activity of the APC, thereby preventing cell cycle progression [43,45] (reviewed in [47,48]). The novel MAD2β, which interacts with

the cytotail of MDC9, has significant sequence similarity to MAD2 and is ubiquitously transcribed. It will therefore be interesting to determine whether MAD2β has a similar role to MAD2's in regulating cell cycle progression. However, MAD2β's function might be unique to higher eukaryotes because no apparent orthologue is present in the *Saccharomyces cerevisiae* genome database.

In evaluating the potential functional significance of the observed interactions, several explanations are possible. First, TACE might be involved in modulating certain aspects of the cell cycle. In this model, TACE might regulate MAD2 function directly or indirectly, for example by sequestering it and thus affecting its availability. Alternatively, TACE might function downstream of MAD2 in the mitotic checkpoint pathway. Secondly, the binding of MAD2 might have a role in regulating TACE function in a cell-cycle-dependent manner. Similar arguments to those outlined above for the interaction between MAD2 and TACE could be made for the function of MAD2β with respect to MDC9, if MAD2β is also found to have a role in regulating cell cycle progression.

Lastly, MAD2 and/or MAD2β might be linked to metalloprotease–disintegrin activity in a manner that is independent of the cell cycle. Consistent with this idea is the report that MAD2 also binds to the insulin receptor [37]. Stimulating cells with insulin decreases the interaction of MAD2 with the insulin receptor, suggesting that MAD2 favours an interaction with the resting rather than the active insulin receptor [37]. Additionally, Petersen et al. [49] have demonstrated that in *Schizosaccharomyces pombe* MAD2 is required for maintaining mating competence in the presence of microtubule-destabilizing agents and that this function is in addition to a role of MAD2 in the mitotic checkpoint. If MAD2 does indeed have additional functions, it is possible that these might depend on the state of microtubule polymerization or depolymerization in the cell.

In summary, we report the identification of candidate cytoplasmic binding partners of the metalloprotease–disintegrins TACE and MDC9. The intriguing finding that two structurally related proteins, MAD2 and MAD2β, were independently identified as interacting partners of distinct metalloprotease–disintegrins raises the question of whether MAD2 and MAD2β are involved in modulating metalloprotease–disintegrin function. These results suggest the possibility that either MAD2 and MAD2β have functions that are not directly related to the cell cycle or that there might be a link between the cell cycle and the function of metalloprotease–disintegrins.

Note added in proof (received 22 September 1999)

The cDNA sequence and chromosomal localization of MAD2β has recently been determined by Cahill et al. [50].

We thank Dr. L. Howard and Dr. G. Weskamp for generating various MDC cytotail constructs; Dr. K. Wassman, Dr. Y. Li and Dr. R. Benezra for hsMAD2 constructs and anti-MAD2 antibodies; Dr. J. D. Becherer for the full-length cDNA clone of human TACE; and members of the Blobel lab and Dr. R. Benezra for comments on the manuscript. This work was supported in part by National Institutes of Health Grant R55GM51988 (to C.P.B.), by a grant from Glaxo Wellcome (to C.P.B.), by a National Institute of Health National Research Service Award 5F32GM18585-02 (to K.K.N.), by a National Institutes of Health Training Grant 5T32GM07739-17 and the Louis and Rachel Rudin Family Foundation (to J.S.), by the Memorial Sloan-Kettering Cancer Center Support Grant NCI-P30-CA-08748 and by the DeWitt Wallace Fund for MSKCC.

REFERENCES

1 Wolfsberg, T. G. and White, J. M. (1996) Dev. Biol. **180**, 389–401
2 Blobel, C. P. (1997) Cell **90**, 589–592
3 Black, R. A. and White, J. M. (1998) Curr. Opin. Cell Biol. **10**, 654–659
4 Primakoff, P., Hyatt, H. and Tredick-Kline, J. (1987) J. Cell Biol. **104**, 141–149
5 Blobel, C. P., Wolfsberg, T. G., Turck, C. W., Myles, D. G., Primakoff, P. and White, J. M. (1992) Nature (London) **356**, 248–252
6 Blobel, C. P., Myles, D. G., Primakoff, P. and White, J. W. (1990) J. Cell Biol. **111**, 69–78
7 Myles, D. G., Kimmel, L. H., Blobel, C. P., White, J. M. and Primakoff, P. (1994) Proc. Natl. Acad. Sci. U.S.A. **91**, 4195–4198
8 Evans, J. P., Schultz, R. M. and Kopf, G. S. (1995) J. Cell Sci. **108**, 3267–3278
9 Evans, J. P., Schultz, R. M. and Kopf, G. S. (1997) Dev. Biol. **187**, 94–106
10 Evans, J. P., Kopf, G. S. and Schultz, R. M. (1997) Dev. Biol. **187**, 79–93
11 Shilling, F. M., Kratzschmar, J., Cai, H., Weskamp, G., Gayko, U., Leibow, J., Myles, D. G., Nuccitelli, R. and Blobel, C. P. (1997) Dev. Biol. **186**, 155–164
12 Cho, C., Bunch, D. O., Faure, J. E., Goulding, E. H., Eddy, E. M., Primakoff, P. and Myles, D. G. (1998) Science **281**, 1857–1859
13 Almeida, E. A. C., Huovila, A.-P. J., Sutherland, A. E., Stephens, L. E., Calarco, P. G., Shaw, L. M., Mercurio, A. M., Sonnenberg, A., Primakoff, P., Myles, D. G. and White, J. M. (1995) Cell **81**, 1095–1104
14 Chen, M. S., Almeida, E. A. C., Huovila, A.-P. J., Takahashi, Y., Shaw, L. M., Mercurio, A. M. and White, J. M. (1999) J. Cell Biol. **144**, 549–561
15 Yagami-Hiromasa, T., Sato, T., Kurisaki, T., Kamijo, K., Nabeshima, Y. and Fujisawa-Sehara, A. (1995) Nature (London) **377**, 652–656
16 Fambrough, D., Pan, D., Rubin, G. M. and Goodman, C. S. (1996) Proc. Natl. Acad. Sci. U.S.A. **93**, 13233–13238
17 Rooke, J., Pan, D., Xu, T. and Rubin, G. M. (1996) Science **273**, 1227–1230
18 Pan, D. and Rubin, J. (1997) Cell **90**, 271–280
19 Sotillos, S., Roch, F. and Campuzano, S. (1997) Development **124**, 4769–4779
20 Wen, C., Metzstein, M. M. and Greenwald, I. (1997) Development **124**, 4759–4767
21 Peschon, J. J., Slack, J. L., Reddy, P., Stocking, K. L., Sunnarborg, S. W., Lee, D. C., Russell, W. E., Castner, B. J., Johnson, R. S., Fitzner, J. N. et al. (1998) Science **282**, 1281–1284
22 Black, R., Rauch, C. T., Kozlosky, C. J., Peschon, J. J., Slack, J. L., Wolfson, M. F., Castner, B. J., Stocking, K. L., Reddy, P., Srinivasan, S. et al. (1997) Nature (London) **385**, 729–733
23 Moss, M. L., Jin, S.-L. C., Milla, M. E., Burkhart, W., Cartner, H. L., Chen, W.-J., Clay, W. C., Didsbury, J. R., Hassler, D., Hoffman, C. R. et al. (1997) Nature (London) **385**, 733–736
24 Buxbaum, J. D., Liu, K. N., Luo, Y., Slack, J. L., Stocking, K. L., Peschon, J. J., Johnson, R. S., Castner, B. J., Cerretti, D. P. and Black, R. A. (1998) J. Biol. Chem. **273**, 27765–27767
25 Merlos-Suarez, A., Fernandez-Larrea, J., Reddy, P., Baselga, J. and Arribas, J. (1998) J. Biol. Chem. **273**, 24955–24962
26 Izumi, Y., Hirata, M., Hasuwa, H., Iwamoto, R., Umata, T., Miyado, K., Tomai, Y., Kurisaki, T., Sehara-Fujisawa, A., Ohno, S. and Mekada, E. (1998) EMBO J. **17**, 7260–7272
27 Gearing, A. J. H., Beckett, M., Christodoulou, M., Churchhill, M., Clements, J., Davidson, A. H., Drummond, A. H., Galloway, W. A., Gilbert, R., Gordon, J. L. et al. (1994) Nature (London) **370**, 555–558
28 McGeehan, G. M., Becherer, J. D., Bast, Jr., R. C., Boyer, C. M., Champion, B., Connolly, K. M., Conway, J. G., Furdon, P., Karp, S., McElroy, A. B. et al. (1994) Nature (London) **370**, 558–561
29 Roghani, M., Becherer, J. D., Moss, M. L., Atherton, R. E., Erdjument-Bromage, H., Arribas, J., Blackburn, R. K., Weskamp, G., Tempst, P. and Blobel, C. (1999) J. Biol. Chem. **274**, 3531–3540
30 Li, Y. and Benezra, R. (1996) Science **274**, 246–248
31 Chen, R. H., Waters, J. C., Salmon, E. D. and Murray, A. W. (1996) Science **274**, 242–246
32 He, X., Patterson, T. E. and Sazer, S. (1997) Proc. Natl. Acad. Sci. U.S.A. **94**, 7965–7970
33 Li, R. and Murray, A. W. (1991) Cell **66**, 519–531
34 Krätzschmar, J., Lum, L. and Blobel, C. P. (1996) J. Biol. Chem. **271**, 4593–4596
35 Lum, L., Reid, M. S. and Blobel, C. P. (1998) J. Biol. Chem. **273**, 26236–26247
36 Weskamp, G., Krätzschmar, J. R., Reid, M. and Blobel, C. P. (1996) J. Cell Biol. **132**, 717–726
36a Howard, L., Nelson, K. K., Maciewicz, R. A. and Blobel, C. P. (1999) J. Biol. Chem., in the press
37 O'Neill, T. J., Zhu, Y. and Gustafson, T. A. (1997) J. Biol. Chem. **272**, 10035–10040
38 Jin, D.-Y., Spencer, F. and Jeang, K.-T. (1998) Cell **93**, 81–91
39 Kim, S. H., Lin, D. P., Matsumoto, S., Kitazono, A. and Matsumoto, T. (1998) Science **279**, 1045–1047
40 Hwang, L. H., Lay, L. F., Smith, D. L., Mistrot, C. A., Hardwick, K. G., Hwang, E. S., Amon, A. and Murray, A. W. (1998) Science **279**, 1041–1044
41 Chen, R.-H., Shevchenko, A., Mann, M. and Murray, A. W. (1998) J. Cell Biol. **143**, 283–295

42 Waters, J. C., Chen, R.-H., Murray, A. W. and Salmon, E. D. (1998) J. Cell Biol. **141**, 1181–1191
43 Li, Y., Gorbea, C., Mahaffey, D., Rechsteiner, M. and Benezra, R. (1997) Proc. Natl. Acad. Sci. U.S.A. **94**, 12431–12436
44 Wassmann, K. and Benezra, R. (1998) Proc. Natl. Acad. Sci. U.S.A. **95**, 11193–11198
45 Fang, G., Yu, H. and Kirschner, M. W. (1998) Genes Dev. **12**, 1871–1883
46 Kallio, M., Weinstein, J., Daum, J. R., Burke, D. J. and Gorbsky, G. J. (1998) J. Cell Biol. **141**, 1393–1406
47 Hardwick, K. G. (1998) Trends Genet. **14**, 1–4
48 Elledge, S. J. (1998) Science **279**, 999–1000
49 Petersen, J., Heitz, M. J. and Hagan, I. M. (1998) Curr. Biol. **8**, 963–966
50 Cahill, D. P., da Costa, L. T., Carson-Walter, E. B., Kinzler, K. W., Vogelestein, B. and Lengauer, C. (1999) Genomics **58**, 181–187

Received 28 April 1999/12 July 1999; accepted 31 August 1999